The LVD signals during the early-mid stages of the L'Aquila seismic sequence and the radon signature of some aftershocks of moderate magnitude

Published version:

DOI:10.1016/j.jenvrad.2014.09.017

(Article begins on next page)

Cigolini C., Laiolo M., Coppola D. (2014) The LVD signals during the early-mid stages of the L'Aquila seismic sequence and the radon signature of some aftershocks of moderate magnitude. Journal of Environmental Radioactivity, 139,56-65. http://dx.doi.org/10.1016/j.jenvrad.2014.09.017

The LVD signals during the early-mid stages of the L'Aquila seismic sequence and the radon signature of some aftershocks of moderate magnitude

Cigolini C.[1,2], Laiolo M.[1,3], Coppola D.[1]

1 – Dipartimento di Scienze della Terra, Università di Torino,Via Valperga Caluso 35, 10125 Torino, Italy
2 –NatRisk, Centro Interdipartimentale sui Rischi Naturali in Ambiente Montano e Collinare, Università degli Studi di Torino, Italy
3 – Dipartimento di Scienze della Terra, Università di Firenze, Via Giorgio La Pira 4, 50121 Firenze, Italy

Correspondig Author: Corrado Cigolini
Email: corrado.cigolini@unito.it; Phone: +39-011670-5107; Fax: +39-011670-5128

***Highlights (for review)**

Highlight

1) The April 9, 2009 Aquila earthquake (ML 5.9) had a remarkable echo in the media
2) We report LVD traces together with the data of a radon monitoring experiment
3) Radon emissions were measured by 3 automatic stations along the main NW-SE fault
4) The one that better responds to seismicity was placed in the fault's bedrock
5) Future networks for earthquake radon monitoring should implement this setting

The LVD signals during the early-mid stages of the L'Aquila seismic sequence and the radon signature of some aftershocks of moderate magnitude

Cigolini C.[1,2], Laiolo M.[1,3], Coppola D.[1]

1 – Dipartimento di Scienze della Terra, Università di Torino,Via Valperga Caluso 35, 10125 Torino, Italy
2 –NatRisk, Centro Interdipartimentale sui Rischi Naturali in Ambiente Montano e Collinare, Università degli Studi di Torino, Italy
3 – Dipartimento di Scienze della Terra, Università di Firenze, Via Giorgio La Pira 4, 50121 Firenze, Italy

Correspondig Author: Corrado Cigolini
Email: corrado.cigolini@unito.it; Phone: +39-011670-5107; Fax: +39-011670-5128

Key words: *LVD traces, radon monitoring, earthquake precursors, networks for radon monitoring*

Abstract

The L'Aquila seismic swarm culminated with the mainshock of April 6, 2009 (M_L=5.9). Here, we report and analyze the Large Volume Detector (LVD, used in neutrinos research) low energy traces (~0.8 MeV), collected during the early-mid stages of the seismic sequence, together with the data of a radon monitoring experiment. The peaks of LVD traces do not correlate with the evolution and magnitude of earthquakes, including major aftershocks. Conversely, our radon measurements obtained by utilizing three automatic stations deployed along the regional NW-SE faulting system, seem to be, in one case, more efficient. In fact, the timeseries collected on the NW-SE Paganica fracture recorded marked variations and peaks that occurred during and prior moderate aftershocks (with M_L>3). The Paganica monitoring station (PGN) better responds to active seismicity due to the fact that the radon detector was placed directly within the bedrock of an active fault. It is suggested that future networks for radon monitoring of active seismicity should preferentially implement this setting.

Introduction

The L'Aquila seismic swarm affected the Abruzzo region in Central Italy since December 2008 to September 2009 (Fig. 1). During the seismic sequence a major earthquake hit the city of Aquila on April 6 of that year (at 01:32 UTC) causing 309 victims (Amato et al., 2011). The magnitude of the event was rated ML 5.9 on the Richter scale with a moment magnitude Mw 6.3. In the light of this parameter this was the ninth stronger earthquake since the beginning of the XXth century (Table 1). Several thousand foreshocks and aftershocks were recorded by the Istituto Nazionale di Geofisica e

Vulcanologia (INGV), and more than 30 events had a magnitude higher than 3.5 (Chiaraluce et al., 2011). Major aftershocks occurred on April 7 and April 9, with magnitudes (M_L) of 5.3 and 5.1, respectively.

Fig. 1 and Table 1

The major earthquake was triggered by the motion of a NW-SE trending normal fault parallel to the trending of the Apennines central axis (Akinci et al., 2009; Herrmann et al., 2011). The depth of the hypocenter was estimated to be at about 9.5 km (Latitude 42.3476°N, Longitude13.3800 E; Chiaraluce et al., 2011 among others). The central part of the Apennines has been characterized by extensional tectonics since Pliocene times due to the faster opening of the back-arc basin (Tyrrhenian sea) compared with the rates of plate convergence, the latter associated with the collision of the Adria microplate with the major Eurasian plate. (e.g., Riguzzi et al., 2013).

The Aquila earthquake had a remarkable echo in the media due to the fact that G. Giuliani claimed that he could have predicted, by means of radon data, the April 6, 2009 earthquake (cf. its reconstruction of the events summarized in an informative monograph: Giuliani, 2009). Within the same year, the International Commission on Earthquake Forecasting for Civil Protection, after interviewing him, concluded, also in the light of the available geophysical data collected by other groups of scientists, that there were “no convincing evidence of diagnostic precursors” of the mainshock before its occurrence (Jordan et al., 2009, p. 323 and p. 361). An additional issue on the Aquila earthquake is related to the fact that seven experts were each sentenced “for downplaying seismic risk” before the occurrence of the deadly event (Cartlidge, 2014). Currently, an appeal on this case is pending.

Beside radon, several other signals, some of them precursory, were reported after the main event, such as earthquake lights (Fidani, 2010), variations in the intensity of radio waves in the LF and VLF bands (Biagi et al., 2009; Rozhnoi et al., 2009), thermal anomalies onto seismogenetic areas

(Pergola et al., 2010; Genzano et al., 2009), small mud volcanoes in the Aterno valley (De Martini et al., 2012), "storms of crustal stress" and acoustic emissions (Gregori et al., 2010), electric field anomalies (Fidani, 2010), and uranium (U) groundwater anomalies (Plastino et al., 2010).

In addition, Bonfanti et al. (2012) discussed the relationships between seismicity and CO_2 - CH_4 degassing during the main seismic sequences that affected Central Appenines within the last two decades. However, several authors emphasized the possible role of "large-scale pockets of high fluid pressure" in the triggering of l'Aquila seismic sequence (Terakawa et al., 2010), as well as the one of Colfiorito, during 1996-1997 (Di Luccio et al., 2010, Lucente et al., 2010). Moreover, Chiodini et al. (2011) found an increase of radiogenic isotopes of crustal origin (^{4}He and ^{40}Ar) in local water tables, likely related to the structural setting of the region.

However, Pulinets et al. (2009) suggested a correlation between the ionization of the near ground layer of the atmosphere and radon emissions at l'Aquila (since its decay products may become clusters for water condensation and local temperature anomalies as suggested by Ouzounov and Freund, 2004).

Radon is radioactive gas generated from the decay of uranium bearing rocks, soils and magmas. The role of radon as a potential precursor of earthquake has been extensively debated. It is generally accepted that anomalous radon emissions, together with those of other geochemical and geophysical parameters, may be released prior an earthquake (Toutain and Baubron, 1999; Kumar et al., 2009). Peaks in radon concentrations before, during and after the onset of tectonic earthquakes (up to 1200 % background values) have been reported in literature since the early sixties (Cicerone et al., 2009). Radon is also considered as an indicator of crustal stress regimes (e.g., Steinitz et al, 2003; Trique et al., 1999). In summary, the radon-earthquake relationships can be correlated to stress regimes, fracturing and microfracturing of crustal rocks (e.g., Hishimuma et al., 1999; Tuccimei et al., 2010) in preparing the ground for the development of a seismic event, during its onset and/or after its occurrence.

In nature, radon is essentially present as ^{222}Rn (with a half life of 3.82 days) and its anomalies were observed before, during and after the onset of regional seismic events (e.g., Scholtz et al., 1973; Fleischer and Mogro-Campero, 1985; Igarashi et al., 1995; Richon et al, 2003; Planinić et al., 2004; Crockett et al., 2006; Kawada et al., 2007; Ghosh et al., 2009; Cigolini, 2010). Variations in radon emissions were also observed during changes in volcanic activity and volcanically-related earthquakes at Hawaii (Cox, 1980; Thomas et al., 1986). Cigolini et al. (2001) were able, by utilizing a network of measuring stations at Mount Vesuvius, to discriminate ^{222}Rn anomalies due to regional earthquakes from those related to volcanic seismicity. However, Burton et al. (2004) performed systematic radon measurements at Mount Etna (during the seismic sequence of October, 2002) and decoded the trend and extension of a hidden fault. Relationships between seismogenic faults and radon emissions have been recently investigated by several authors (Vaupotiĉ et al., 2010; Papastefanou, 2010), whereas Reddy et al. (2004) found a correlation between the increase of radon concentrations and microseismicity in a stable continental region. Moreover, Cigolini et al. (2007) detected earthquake-volcano interactions at Stromboli volcano: in this case radon anomalies were precursory, coseismic and somehow delayed in respect to the onset of regional seismic events. However, the anomalies of radon signal are better suited to forecast eruptive episodes since we know the loci of volcanic eruptions and we can follow the evolution of volcanic activity (e.g., Chirkov, 1975; Connors et al., 1996; Alparone et al., 2005; Cigolini et al., 2005; 2013). Conversely, its role as a precursor of earthquakes is more controversial since we do not know when and where the earthquake is going to hit.

Several works show that environmental parameters are critical in modulating radon emissions (e.g., Mogro-Campero and Fleischer, 1977; Pinault and Baubron, 1996; Planinić et al., 2001; Pérez et al., 2007; Cigolini et al., 2009). Automatic and real-time measurements substantially increase the potential role of radon in earthquake prediction since the data are may be easily collected, transferred, elaborated and filtered thus minimizing the interference of environmental parameters

(Cigolini et al., 2009; Laiolo et al., 2012). Therefore, time series analysis of the ^{222}Rn signal allow us to better track radon degassing in space and time.

In this paper we are revisiting some Large Volume Detectors (LVD) data collected at the "Laboratori Nazionali del Gran Sasso, LNGS" (Gran Sasso National Laboratories) in the attempt to infer radon variations during the evolution of the seismic sequence. LVD are large volume liquid scintillator detectors created to search for neutrinos from gravitational stellar collapses in our galaxy (LVD Collaboration, 1992; 2005). It is well known that there is a rather remarkable correlation between the background signal of these detectors and the alpha decays due to ^{222}Rn (e.g., Bruno and Meghetti, 2006). In addition, we will present some the data of an experiment on radon monitoring in the area that recorded the effects of few aftershocks with M_L>3.

Methods

Details on the type and functioning of LVD detector are extensively given in LVD Collaboration (1992; 2005). Here, we summarize the main technical features and principles (cf. also Anzivino et al., 1993 for details on the electronics).

Single LVD detectors consist of an active scintillator mass of 1000 t constructed in stainless still counters (1.5 m^3 each in volume, with walls of 4 mm thick). Currently an array of 840 scintillators is deployed in a compact and modular geometry. Additionally, counters are shielded by iron layers from 1.5 cm to 2 cm in thickness. Neutrinos detections occurs by counting the inverse beta decay reaction of electron anti-neutrinos on scintillator protons followed by the neutron capture. External counters (43%) operate at energy threshold Eh ~ 7 MeV, whereas the inner ones (57%) run at Eh ~4 MeV and are better shielded from rock radioactivity. Counters are equipped with an additional refinement channel, set at a lower threshold El ~ 0.8 MeV to record γ pulses. Thus, every ten minutes the low threshold counting rate of each counter is activated (within a time window of 10 seconds) to measure the background at the low energy threshold. This background is essentially related to the nuclear decays of ^{238}U, ^{232}Th and ^{40}K present in the surrounding rocks and environmental radon; secondary neutral particles generated in muon interaction with the rocks or within detector's materials may also contribute to background levels. Recently, Bruno and Menghetti (2006) concentrated their work on low energy signals and found a remarkable correlation between the LVD counting rates and those obtained by a alpha particles radon-meter (with a relative error of about 10% at 95% confidence levels) (Fig. 2). In particular, they retrieved a linear relationship of this type, for LVD counts being comprised between 40 and 75

$$C_{Rn}\left[Bq/m^3\right] = 7LVD_{cts} - 290 \qquad (1)$$

so that, within this range, a 1 count/sec step measured at LVD is roughly equivalent to a 7 Bq/m^3 in terms of radon activity. They pointed out that there is a time delay between the LVD data and those of radon due to the higher efficiency of γ counts in respect to the α counts associated with the radon decay chain. Moreover, they showed that the opening of the Gran Sasso National Laboratories during working hours modulates concordantly the LVD and the radon signal due to air ventilation, leading to daily fluctuations up to about 200 Hz (cf. Fig. 2). These effects in tunnels and underground openings have been also described by Richon et al. (2009) and Eff-Darwich et al. (2002; 2008). Obviously these fluctuations may somehow effect the peak geometry of the recorded timeseries. Previous works on radon emissions within these laboratories were performed by Plastino and Bella (2001), Plastino et al. (2009).

Fig. 2

We installed three automatic radon monitoring stations at selected sites along the NE-SW Appenine major faults by utilizing three DOSEman electronic radon sensors (produced by SARAD Gmbh). One was deployed along the Paganica fracture, one at the Capannelle Pass and the third was located near the village of Aringo, at about 25 km NNE of L'Aquila (see Fig. 3).

Fig. 3

In these detectors, the radon gas diffuses through a leather membrane into a cylindrical measurement chamber (12 cm^3 in volume); here the charged alpha particles interact with a Si-doped semiconductor detector and are counted by an automated electronic spectrometer. The counts are stored and instantaneously processed by a multichannel analyser that splits them into discrete energetic domains, known as Regions of Interest (ROIs), thus the spectrum of the radon and its progeny can be reconstructed (Fig. 4). The sensitivity of these detectors covers the range 10 Bq/m^3 to 4 millions of Bq/m^3.

Each single DOSEman detector, used during our experiment, was carefully calibrated within a "radon chamber" to measure the alpha particles within delimited energy windows. In particular, the Paganica station and the Capannelle station measured within 4410-9555 keV and 4830-9875 keV, respectively, whereas the Aringo station was measuring between 4620-9765 keV (Fig. 4). These windows include the peaks of ^{222}Rn and its progeny (^{218}Po, ^{214}Po) together with ^{220}Rn, thoron (the latter related to the decay of the ^{232}Th chain). However, Gründel and Postendörfer (2003; p. 290) emphasized that the counts for ^{214}Po need to be corrected due to the fact that the higher side of the ^{220}Rn spectrum somehow overlaps the ^{214}Po peak. Thus, they suggested that 7.5 % of the counts of the latter may be due to thoron.

Fig. 4

Appropriate radon activities in Bq/m^3 can be computed from the total counts of single ROIs (within a given sampling-time: 6 hours in our case) by means of the following relationship (Streil et al., 2002; Gründel and Postendörfer, 2003):

$$\mathrm{C_i}\left[\mathrm{Bq/m^3}\right] = \left(C_{f_i} / Cts * \left(1/t_s\right)\right) * 1000 \qquad (2)$$

where C_{fi} is calibration factor of the instrument (linked to the chamber volume) *Cts* are the counts, t_s is the sampling time (in minutes) and 1000 is the conversion factor from kBq/m^3 to Bq/m^3. Radon can be computed in *fast mode* counting ^{222}Rn and ^{218}Po only, or *slow mode* that includes the counts of ^{214}Po as well. The reported data were obtained by utilizing the "fast mode" option since ^{214}Po may combine with resident moisture particles, plus we don't have to take into account thoron interferences (on the ^{214}Po peaks). The new generation of DOSEman detectors have instrumental uncertainties, for radon concentrations at 1,000 Bq/m^3 of about 10%, drastically decreasing at higher emissions. We also included, within the Paganica station a temperature data logger (Testo 905-T2) to record the soil temperatures a with sample time of 1 hour, since this parameter is crucial in better interpreting the radon signal (Iskandar et al., 2004).

Earlier studies (Bellotti et al., 2007) have shown that in the Abruzzo region there are no particular risks regarding the presence of radiogenic rocks and/or soils. Indoor measurements average 60 Bq/m^3, whereas peak values have only been recorded in the central part of l'Aquila province (up to about 1100 Bq/m^3). Systematic soil measurements give mean ^{238}U concentrations of 2.5 ppm (Sarra et al., 2012) with radon concentrations approaching 25 Bq/kg, under the assumption that secular equilibrium conditions are reached (Parks et al., 2013).

LVD data during early-mid stages of the l'Aquila seismic sequence

We hereby present and analyze the LVD data collected from March 2 to May 1, 2009 at the Gran Sasso National Laboratories near the village of Assergi, located at 15 km NE of l'Aquila (Fig. 5). Then we compare some of our data with LVD traces during the aftershocks that occurred during our monitoring experiment. We have also included the timeseries of events with M_L>2 as well as the histograms of the total number of earthquakes (above the cited reference magnitude) during the evolution of the seismic swarm. More reliable LVD data are those evidence by gray bands that refer to the weekly closure of the laboratories. Among these we have those of March 28-30 and April 4-5 that preceded the mainshock of April 6. It can be easily seen that there is no clear peak in LVD counts prior the foreshocks of March 30, with two events reaching a magnitude M_L of about 4. Similarly, the peak that preceded the major earthquake of April 6 reaches a value of 50 counts and its height is minor in comparison of the fluctuations present in the whole dataset. However, after the mainshock there is an increase in LVD counts that reach 55 counts/sec. The major aftershocks (of April 7 and April 9, with ML 5.3 and ML 5.4, respectively) occur during a descending trend in LVD counts. During this span of time the labs were obviously closed for safety reasons. In this period the signal is more stable than earlier and increase to 58 counts by April 11 likely due to the enhanced fracturing associated with the aftershocks. Then a decreasing trend is recorded with one discontinuity on April 14 followed by a relatively stable signal until the sharp increase (but relatively low in counts: 52) during the early hours of April 19 which is not accompanied or followed by any significant seismic event, and the number of earthquakes falls below 5 per day. A nearly similar peak (in counts) occurs during the evening of April 22 (53 counts/sec) and precede the two events of April 23 with $M_L > 4$. The major peak of April 27 is not correlated with any M_L 3-4 event and is probably associated with an increase in microseismicity. Finally the peak of May 1 seems to be postseismic to the 3.8 M_L event and a moderate increase in the number of earthquakes.

Fig. 5

Radon measurements during the mid stages of the l'Aquila seismic sequence

In Fig. 6 we report the data collected during our experiment at three selected sites. One was located along the Paganica fracture that runs parallel to the regional NE-SW faulting system, one at the Capannelle pass and the third was located near the village of Aringo, i.e. the northeastern edge of our prospecting area.

The Paganica station was deployed at about 3 km NW of the village just below the soil-rock interface (at a depth of about 70 cm) that separates the colluvium deposits from the upper Cretaceous calcarenites and breccias that outcrop in the area. The Capannelle station was inserted into the thick colluvium soil (at a depth of 1 m) that overlays the lower Cretaceous limestones of the "Maiolica" Formation. Finally, the Aringo station was inserted at a depth of 1m in the colluvium soil that covers the upper Miocene sandstones and mudstones ("Flysch della Laga"), at a distance of about 2 km, NW of the village of Aringo.

The Paganica station shows an overall increasing trend in radon emissions reaching 830 Bq/m^3 and an average of 600 ± 350 Bq/m^3 during the exposure time. In this section we simply compare these measurements with those obtained at the other two sites, and will be better describe the timeseries recorded at Paganica in the following section.

The radon signal at Capannelle station is more fluctuating in terms of radon concentration an we may easily recognize two periods with higher ^{222}Rn emissions. The first one, of April 24 2009 being postseismic to an event of magnitude M_L=4, with radon reaching 1100 Bq/m^3. Then radon concentrations moderately decrease and fluctuate nearly above 500 Bq/m^3 until the afternoon of April 26 likely due to the abundance of earthquakes above M_L>3 (nine of them were recorded). In the following days the radon signal decreases together with active seismicity. Until April 28 the radon signal is low ~400 Bq/m^3, and we only have 4 earthquakes that reach M_L= 3 or slightly higher. It is interesting to note that radon increases after the onset of two events (in the morning of April 28) approaching to M_L~3 (together with a time gap in the release of seismic energy with M_L>2) until it reaches a relative maximum up to 1150 Bq/m^3. Then the signal moderately decreases during April 29 when the total amounts of event has only a moderate increase (from 100 to 130 per day). Moreover, there are no particular peaks before the seismic event of May 1, that reaches a magnitude M_L=3.8.

Fig. 6

Finally the radon signal for the Aringo station is somehow higher in terms of radon concentration being up to 1600 Bq/m^3, with an average of 1000 ± 150 Bq/m^3. In this case the signal is rather noisy and fluctuating and there is no apparent correlation with active seismicity. This is probably due to the thick colluvium cover and the nature of the basement rocks that attenuated the vibrations associated with seismic transients. It is not excluded that the irregular topography in the surroundings of the station made this site more vulnerable to the effects of environmental parameters.

Fig. 7

Insights on radon emissions at the Paganica Station

We hereby report the full data set recorded at the Paganica station which seems to be more reliable due to the fact that was inserted within the bedrock just below the soil-rock interface and seems to better respond to seismic shaking (e.g., Perrier et al., 2013). This has also been operative for a longer time essentially for logistic reasons. In particular, this station has been deployed directly onto the fracture zone whose activation caused the major damages in the nearby village during the mainshock of April 6, 2009. The reported timeseries (Fig. 7) show a rather persistent increase in radon emissions that fluctuate around mean values. Fluctuation in the signal seem to be related to changes in environmental parameters, such as soil and air temperatures and atmospheric pressure that affect radon transfer toward the surface. Meteorological data were acquired, as daily averages, from the metereological station at Ponte San Giovanni (Fig. 8). In Table 2 we report the correlation coefficients between the daily averages of radon emissions and the environmental parameters (soil and air temperatures, atmospheric pressures, air humidity and rain).

Fig. 8 and Table 2

Conversely to what observed in volcanic areas (such as Stromboli and Etna, cf. Laiolo et al., 2012; Morelli et al., 2006), here we have a positive correlation of radon emissions with increasing soil and air temperatures. This peculiarity was already observed, since temperature may affect the emanation factor of radon from under laying rocks (Iskandar et al., 2004; Girault et al., 2011), thus giving higher radon emissions (cf. Finkelstein et al., 2006).

Increasing radon concentrations occur more clearly since May 5, 2009, being essentially correlated with a progressively higher number of daily earthquakes. This is also proved by the Multiple Linear Regression Analysis used to graphically minimize the effects of the cited environmental parameters on the raw radon signal (cf. Laiolo et al., 2012). The results indicate the influence of temperature with the residuals of radon emissions, whereas other environmental parameters do not particularly affect the cited signal (cf. Table 2).

Fig. 9

However, the trend of the residuals, reported in Fig. 9, still maintains rather visible fluctuations.

To have a better picture of these variations we used a graph that reports the time series of the residuals compared with the magnitude of aftershocks with $M_L>2$ that occurred during the time span of our experiment (Fig. 10). Major variations occur on May 1, being essentially coseismic with the onset of an aftershock of $M_L=3.8$ (at 5:12 GMT) when ^{222}Rn drops down to 260 Bq/m^3 . Another drastic variation is the one that precedes of about 12 hours the event of May 14, 2009 (at 6:30 GMT) that shows a similar magnitude and radon reaches a relative maximum of 1220 Bq/m^3. The epicentral distance of the above earthquakes was respectively 3 and 18 km (a sketch of aftershocks location is shown in Fig. 11). It is interesting to point out that the latter aftershock is the only one that shows, within the span of time of our monitoring, a focal mechanism of a typical *pure normal fault*. All other earthquakes show oblique components due to shearing.

Fig. 10 and Fig. 11

In general, fluctuation of the radon signal do not seem to be correlated with other particular seismic events of lower magnitude.

Discussion and conclusions

The Aquila seismic sequence has demonstrated the limits of the potential role of radon as earthquake precursor, particularly if radon emissions are monitored at single sites without taking into account the local geology. With no doubt radon anomalies may be precursors of major seismic events but may also be coseismic, postseismic and/or related to microseismicity (cf., Reddy et al., 2004). However, this has been a rather debated issue in recent years (e.g., Wyss, 1991; 1997; Wakita, 1996; Nature debates, 1999; Planinić et al., 2004; Zmazek et al., 2005; Immè and Morelli, 2012). In particular, Planinić et al. (2001) and Zmazek et al. (2005) have discussed the limits of some assumptions at the base of some empirical relationships that correlated radon emissions with the earthquake magnitudes (e.g., Dobrovolsky et al., 1979) without considering the effects of environmental parameters.

In particular, the analysis of the LVD signal has shown that low-energy measurements can be used essentially for assessing the radon background within the Gran Sasso National Laboratories (essentially oriented in evaluating the radon exposure of personnel and related health standards). In fact, there is no evidence of diagnostic peaks in LVD counts before and during the Aquila mainshock of April 6, 2009. However, after this event there is a moderate increase in LVD counts, but major aftershocks (of April 7 and April 9, with M_L 5.3 and M_L 5.4) take place during a decreasing trend in the counts themselves. The reason for these discrepancies are essentially intrinsic to the architectural geometry of tunnels and “chambers” of the laboratories. In particular, the LVD measurements site is within a major hall where the floor is covered by a thick concrete pavement. Moreover, the site is affected by enhanced ventilation during working days and the doors connected with the tunnels are opened rather continuously. An additional issue, strictly geologic, is that the LVD site is not laying onto a regional fault that was activated during the seismic crisis. We may thus conclude that LVD measurements are nor reliable to assess precursory signals related to radon prior and during the occurrence of a seismic sequence.

However, the data collected during our experiment have more complex radon signatures. First, the measuring stations were deployed at a rather low depth (0.7-1 m) and therefore the signal was not stable due to the effects of environmental parameters. However, the radon signal at the Paganica station seems to be more reliable. The reason for its higher efficiency in recording radon variations, before and during seismic aftershocks, seems to be related to the fact that the station was set within the bedrock itself (Upper Cretaceous calcarenites and breccias) that was affected by a major fault actively displaced during the onset of the mainshock.

The other two measuring stations were inserted into thicker colluvial soils that cover bedrock formations and, in this case also, were deployed onto fracture systems that run parallel to the major faults trending NE-SW. In spite of this, the less efficient was the one that inserted into the soil that covers the “softer” arenaceous marls of Flysch della Laga formation. This seems to support the idea that the nature of bedrocks coupled with the position of the radon detector may somehow effect the radon signals which appear, in the latter cases, to be more noisy and randomly fluctuating, thus masking the possible effects of local seismicity (cf. Perrier et al., 2013).

In conclusion, our experiment indicates that particular attention should be given to the choice of the sites for radon measurements. Thus, radon monitoring in seismogenic areas should be undertaken only by measuring the radon signals at sites that are effectively located onto major tectonic structures. In deploying stations we should make sure that the detectors are preferentially placed directly into bedrock units (particularly if these consist of massive rocks that are not radiogenic). Insertion of radon sensors at higher depths could help in minimizing the effects of environmental parameters on the radon signal. Moreover, in placing the measuring stations we should avoid sites where there is a fluctuation of the water bed that may modulate and disturb the radon signal.

In conclusion, we believe that a network for automatic radon measurements opportunely installed could be a starting point for monitoring regional seismicity (Crockett et al., 2006; Papastefanou, 2010). Statistical and more reliable results could be accepted only after few years of continuous measurements along active faults. This would give us a better clue to understand their dynamic behavior, in space and time, before, during and after the onset and development of a seismic crisis.

Acknowledgments

This research has been funded by the Italian Ministry for University and Research (MIUR). We thank Prof. O. Saavedra for making available LVD traces. We are grateful to the Ing. Fabrizio Lombardi and the "AQ Caput Frigoris" association (http://www.caputfrigoris.it) for the metereological data collected from the Ponte S. Giovanni (Scoppito-L'Aquila) station. We are also indebted to the group of the Civil Protection of the "Regione Toscana" for having provided logistic support during our survey at l'Aquila. Prof. M. Fornaro, previous Director of the Department of Earth Sciences at the University of Torino, encouraged us to undertake this research. We also thank the CRT Foundation of Turin for supporting the improvement of our computing system.

References

Akinci A., Galadini F., Pantosti D., Petersen M., Malagnini L., Perkins D., 2009. Effect of Time Dependence on Probabilistic Seismic-Hazard Maps and Deaggregation for the Central Apennines, Italy. Bulletin of the Seismological Society of America April 2009 vol. 99 no. 2A, 585-610, doi: 10.1785/0120080053.

Alparone, S., Behncke, B., Giammanco, S., Neri, M., Privitera, E., 2005. Paroxysmal summit activity at Mt. Etna (Italy) monitored through continuous soil radon measurement. Geophysical Research Letters 2: L16307, doi:10.1029/2005GL023352.

Amato, A., Galli, P., Mucciarelli, M., 2011. Introducing the special issue on the 2009 L'Aquila earthquake. Bollettino di Geofisica Teorica ed Applicata 52 (3), 357-365.

Anzivino, G., Benvenuto, P., Bianco, S., Casaccia, R., Dulach, B., Fabbri, D., Fabbri, F.L., Gatta, M., Giardoni, M., Laakso, I., Lindozzi, M., Passamonti, L., Russo, V., Sarwar, S., Sensolini, G., Ventura, M., Votano, L., Zallo, A., Mencarini, D., Pallante, E., Aftab, Z., Ali, M.M., Chen, K., Chen, R., Cong, S., Cui, X., Ding, H., Gao, B., Li, Y., Lu, L., Minhas, B.K., Shi, Z., Shah, A.R., Sun, Y., Zhou, X., 1993. The LVD tracking system chamber. Nuclear Instruments and Methods in Physics Research A 329, 521-540.

Bellotti, E., Di Carlo, G., Di Sabatino, D., Ferrari, N., Laubenstein, M., Pandola, L., Tomei, C. 2007. γ-ray spectrometry of soil samples from the Provincia dell'Aquila (Central Italy). Applied Radiation and Isotopes 65 (7), 858-865.

Biagi, P. F., Castellana, L., Maggipinto, T., Loiacono, D., Schiavulli, L., Ligonzo, T., Fiore, M., Suciu, E., Ermini, A., 2009. A pre seismic radio anomaly revealed in the area where the Abruzzo earthquake (M=6.3) occurred on 6 April 2009. Natural Hazards Earth System Sciences 9, 1551-1556, doi:10.5194/nhess-9-1551-2009.

Bonfanti, P., Genzano, N., Heinicke, J., Italiano, F., Martinelli, G., Pergola, N., Telesca, L., Tramutoli, V. 2012. Evidence of CO_2-gas emission variations in the central Apennines (Italy) during the L'Aquila seismic sequence (March-April 2009). Bollettino di Geofisica Teorica ed Applicata 53 (1), 147-168.

Bruno G., Menghetti H., 2006. Low energy background measurement (~ 0.8 MeV) with the LVD. Journal of Physics Conference Series 39, 278–280.

Burton, M., Neri, M., Condarelli, D., 2004. High spatial resolution radon measurements reveal hidden active faults on Mt. Etna. Geophysical Research Letters 31 (7), L07618.

Cafagna, F., 2007. Misure di emissioni di radon in diversi contesti geodinamici: i casi del Gran Sasso e di Stromboli. Tesi di Laurea Magistralis in Scienze Geologiche, Dipartimento di Scienze Mineralogiche e Petrologiche, Università degli Studi di Torino, pp. 265.

Cartlidge, E., 2014. Human Activity May Have Triggered Fatal Italian Earthquakes (Emilia), Panel says. Science, 344 no. 6180, 141. doi: 10.1126/science.344.6180.141.

Cafagna, F., 2007. Misure di emissioni di radon in diversi contesti geodinamici: i casi del Gran Sasso e di Stromboli. Tesi di Laurea Magistralis in Scienze Geologiche, Dipartimento di Scienze Mineralogiche e Petrologiche, Università degli Studi di Torino, 265 pp.

Chiaraluce,, L., Chiarabba C., De Gori, P., Di Stefano, R., Improta, L., Piccinini, D., Schlagenhauf, A., Traversa, P., Valoroso, L., Voisin, C., 2011. The 2009 L'Aquila (central Italy) seismic sequence. Bollettino di Geofisica Teorica ed Applicata 52 (3), 367-387

Chiodini, G., Caliro, S., Cardellini, C., Frondini, F., Inguaggiato, S., Matteucci, F., 2011. Geochemical evidence for and characterization of CO2 rich gas sources in the epicentral area of the Abruzzo 2009 earthquakes. Earth and Planetary Science Letters 304 (3–4), 389–398.

Chirkov, A.M., 1975. Radon as a possible criterion for predicting eruptions as observed at Karymsky volcano. Bulletin of Volcanology 39, 126-131.

Cicerone, R.D., Ebel, J.E., Britton, J., 2009. A systematic compilation of earthquake precursors. Tectonophysics 476 (3-4), 371-396.

Cigolini, C., Salierno, G., Gervino, G., Bergese, P., Marino, C., Russo, M., Prati, P., Ariola, V., Bonetti, R., Begnini, S., 2001. High-resolution Radon Monitoring and Hydrodynamics at Mount Vesuvius. Geophysical Research Letters 28 (21), 4035-4039.

Cigolini, C., Gervino, G., Bonetti, R., Conte, F., Laiolo, M., Coppola, D., Manzoni, A., 2005. Tracking precursors and degassing by radon monitoring during major eruptions at Stromboli Volcano (Aeolian Islands, Italy). Geophysical Research Letters 32, L12308 doi:10.1029/2005GL022606.

Cigolini, C., Laiolo, M., Coppola, D., 2007. Earthquake-volcano interactions detected from radon degassing at Stromboli (Italy). Earth and Planetary Science Letters 257, 511-525.

Cigolini, C., Poggi, P., Ripepe, M., Laiolo, M., Ciamberlini, C., Delle Donne, D., Ulivieri, G., Coppola, D., Lacanna, G., Marchetti, E., Piscopo, D., Genco, R., 2009. Radon surveys and real-time monitoring at Stromboli volcano: influence of soil temperature, atmospheric pressure and tidal forces on 222Rn degassing. Journal of Volcanology and Geothermal Research 184(3-4), 381-388.

Cigolini, C., 2010. The dynamics of a double-cell hydrothermal system in triggering seismicity at Somma-Vesuvius: results from a high-resolution radon survey (revisited). Bulletin of Volcanology 72, 693–704.

Cigolini C., Laiolo, M., Ulivieri, G., Coppola, D., Ripepe, M., 2013. Radon mapping, automatic measurements and extremely high 222Rn emissions during the 2002–2007 eruptive scenarios at Stromboli volcano. Journal of Volcanology and Geothermal Research 264, 49- 65.

Connors, C., Hill, B., La Femina, P., Navarro, M., Conway, M., 1996. Soil Rn-222 pulse during the initial phase of the June August 1995 eruption of Cerro Negro, Nicaragua. Journal of Volcanology and Geothermal Research 73, 119-127.

Cox, M.E., 1980. Ground Radon Survey of a Geothermal area in Hawaii. Geophysical Research Letters 7, 283-286.

Crockett, R.G.M., Gillmore, G.K., Phillips, P.S., Denman, A.R., Groves-Kirkby, C.J., 2006. Radon anomalies preceding earthquakes which occurred in the UK, in summer and autumn 2002. Science of the Total Environment 364 (1–3), 138-148.

De Martini, P., Cinti, F., Cucci, L., Smedile, A., Pinzi, S., Brunori, C., Molisso, F., 2012. Sand volcanoes induced by the April 6th 2009 Mw 6.3 L'Aquila earthquake: a case study from the Fossa area. Italian Journal of Geosciences 131 (3), 410-422. doi: 10.3301/IJG.2012.14.

Di Luccio, F., Ventura, G., Di Giovambattista, R., Piscini, A., Cinti, F.R., 2010. Normal faults and thrusts re-activated by deep fluids: the 6 April 2009 Mw 6.3 L'Aquila earthquake, central Italy. Journal of Geophysical Research 115, B06315. doi: 10.1029/2009JB007190.

Dobrovolsky, I.P., Zubkov, S.I., Miachkin, V.I., 1979. Estimation of the size of earthquake preparation zones. Pure and Applied Geophysics 117 (5), 1025-1044.

Dueñas, C., Fernández, M.C., Carretero, J., Liger, E., Pérez, M., 1997. Release of 222Rn from some soils. Annales Geophysicae 15, 124-133.

Eff-Darwich, A., Martín, C, Quesada, M., de la Nuez, J., Coello, J., 2002. Variations on the concentration of 222R in the subsurface of the volcanic island of Tenerife, Canary Islands. Geophysical Research Letters 29, 2069-2073.

Eff-Darwich, A., Viñas, R., Soler, V., de la Nuez, J., Quesada, M.L., 2009. Natural air ventilation in underground galleries as a tool to increase radon sampling volumes for geologic monitoring, Radiation Measurements 43, 1429-1436.

Fidani, C., 2010. The earthquake lights (EQL) of the 6 April 2009 Aquila earthquake, in Central Italy. Natural Hazards Earth System Sciences 10, 967-978. doi:10.5194/nhess-10-967-2010.

Finkelstein, M., Eppelbaum L.V., Price, C., 2006. Analysis of temperature influences on the amplitude frequency characteristics of Rn gas concentration. Journal of Environmental Radioactivity 86, 251–270.

Fleischer, R.L., Mogro-Campero, A., 1985. Association with subsurface radon changes in Alaska and the Northeastern United States with earthquakes. Geochimica and Cosmochimica Acta 49, 1061-1071.

Genzano, N., Aliano, C., Corrado, R., Filizzola, C., Lisi, M., Mazzeo, G., Paciello, R., Pergola, N., and Tramutoli, V. 2009. RST analysis of MSG-SEVIRI TIR radiances at the time of the Abruzzo 6 April 2009 earthquake. Natural Hazards Earth System Sciences 9, 2073-2084. doi:10.5194/nhess-9-2073-2009.

Girault, F., Perrier, F., 2011. Heterogeneous temperature sensitivity of effective radium concentration from various rock and soil samples. Natural Hazards and Earth System Sciences 11, 1619-1626. doi: 10.5194/nhess-11-1619-2011.

Giuliani, G., 2009. L’Aquila 2009 la mia verità sul terremoto. Castelvecchi Editore, Rome, 166 p.

Gregori, G.P., Poscolieri, M., Paparo, G., De Simone, S., Rafanelli, C., and Ventrice, G. 2010. "Storms of crustal stress" and AE earthquake precursors. Natural Hazards and Earth System Sciences 10, 319-337, doi: 10.5194/nhess-10-319-2010.

Ghosh, D., Deb, A., Sengupta, R., 2009. Anomalous radon emission as precursor of earthquake. Journal of Applied Geophysics 69 (2), 67-81.

Gründel, M., Postendörfer. J., 2003. Characterization of an electronic Radon gas personal Dosimeter. Radiation Protection Dosimetry 107 (4), 287–292.

Herrmann, R.B., Malagnini, L., Munafò, I., 2011. Regional Moment Tensors of the 2009 L'Aquila Earthquake Sequence. Bulletin of the Seismological Society of America 101 (3), 975-993. doi: 10.1785/0120100184.

Hishimuma, T., Nishikawa, T., Shimoyama, T., Myajima M., Tamagawa, Y., Okabe, S., 1999. Emission of radon and thoron due to the fracture of rock. Il Nuovo Cimento 22 (3-4), 523-527.

Igarashi, G.: Saeki, S.: Takahata, N.: Sumikawa, K.: Tasaka, S.: Sasaki, Y., Takahashi, M., Sano, Y., 1995. Ground-water Radon Anomaly before the Kobe Earthquake in Japan. Science 269, 60-61.

Immè, G., Morelli, D., 2012. Radon as Earthquake Precursor. In: D'Amico, S., (Eds.), Earthquake Research and Analysis - Statistical Studies, Observations and Planning. InTech Publisher, pp. 143-160. doi: 10.5772/29917 http://www.intechopen.com/books/earthquake-research-and-analysis-statistical-studies-observations-and-planning/radon-as-earthquake-precursor .

Iskandar, D., Yamazawa, H., Iida, T., 2004. Quantification of the dependency of radon emanation power on soil temperature. Applied Radiation and Isotopes 60 (6), 971-973.

Jordan, T.H., Chen, Y.T., Gasparini, P., Madariaga, R., Main, I., Marzocchi, W., Papadopoulos, G., Sobolev, G., Yamaoka, K., Zschau, J. 2011. Final report by the International Commission on Earthquake Forecasting for Civil Protection. Operational Earthquake Forecasting: State of Knowledge and Guidelines for Utilization. Annals of Geophysics 54 (4), 315-391. doi: 10.4401/ag-5350.

Kawada, Y., Nagahama, H., Omori, Y., Yasuoka, Y., Ishikawa, T., Tokonami, S., and Shinogi, M., 2007. Time-scale invariant changes in atmospheric radon concentration and crustal strain prior to a large earthquake. Nonlinear Processes in Geophysics 14, 123–130. http://www.nonlin-processes-geophys.net/14/123/2007.

Kumar, A., Singh, S., Mahajan, S., Bajwa, B.S., Kalia, R., Dhar, S. 2009. Earthquake precursory studies in Kangra valley of North West Himalayas, India, with special emphasis on radon emission. Applied Radiation and Isotopes 67, 1904–1911.

Laiolo, M., Cigolini, C., Coppola, D., Piscopo, D. 2012. Developments in real-time radon monitoring at Stromboli volcano. Journal of Environmental Radioactivity 105, 21- 29.

Lucente, F.P., de Gori, P., Margheriti, L., Piccinini, D., di Bona, M., Chiarabba, C., Agostinetti, N.P. 2010. Temporal variation of seismic velocity and anisotropy before the 2009 Mw 6.3 L'Aquila earthquake, Italy. Geology 38 (11), 1015-1018.

LVD Collaboration, 1992. Il Nuovo Cimento A 105, 1793 p.

LVD Collaboration, 2005. Proc. of the Fifth Int. Workshop on the identification of Dark Matter 471 p.

Mercuri, A., 2009. Terremoti dell'Appenino Centrale e risposta sismica di un generico sito su roccia. Relazioni tra eventi sismici ed emissioni di radon. Tesi di Dottorato in Scienze della Terra (XXI Ciclo). Università degli Studi di Torino, pp. 89.

Morelli, D., Di Martino, S., Immè, G., La Delfa, S., Lo Nigro, S., Patanè G., 2006. Evidence of soil radon as tracer of magma uprising in Mt. Etna. Radiation Measurements 41(6), 721-725.

Mogro-Campero, A., Fleischer, R.L., 1977. Subterrestrial fluid convection: a hypothesis for long distance migration of radon within the earth. Earth and Planetary Science Letters 34, 321-325.

Nature debates, 1999. http://www.nature.com/nature/debates/earthquake/equake_frameset.html

Ouzounov, D., Freund, F.T., 2004. Mid-infrared emission prior to strong earthquakes analyzed by remote sensing data. Advances in Space Research 33 (3), 268-273.

Papastefanou, C., 2010. Variation of radon flux along active fault zones in association with earthquake occurrence. Radiation Measurements 45 (8), 943-951.

Parks, M.M., Caliro, S., Chiodini, G., Pyle, D.M., Mather, T.A., Berlo, K., Edmonds, M., Biggs, J., Nomikou, P., Raptakis, C., 2013. Distinguishing contributions to diffuse CO2 emissions in volcanic areas from magmatic degassing and thermal decarbonation using soil gas Rn^{222}-delta C^{13} systematics: Application to Santorini volcano, Greece. Earth and Planetary Science Letters 377, 180-190.

Pérez, N.M., Hernández, P.A., Padrón, E., Melián, G., Marrero, R., Padilla, G., Barrancos, J., Nolasco, D., 2007. Precursory subsurface ^{222}Rn and ^{220}Rn degassing signatures of the 2004 seismic crisis at Tenerife, Canary Islands. Pure and Applied Geophysics 164, 2431-:2448.

Pergola, N., Aliano, C., Coviello, I., Filizzola, C., Genzano, N., Lacava, T., Lisi, M., Mazzeo, G., Tramutoli, V., 2010. Using RST approach and EOS-MODIS radiances for monitoring seismically active regions: a study on the 6 April 2009 Abruzzo earthquake. Natural Hazards and Earth System Sciences 10, 239-249. doi: 10.5194/nhess-10-239-2010, 2010.

Perrier, F., Girault, F., 2013. Harmonic response of soil radon-222 flux and concentration induced by barometric oscillations. Geophysical Journal International 195 (2), 945-971.

Pinault, J.L., Baubron, J.C., 1996. Signal processing of soil gas radon, atmospheric pressure and soil temperature data: a new approach for radon concentration modeling. Journal of Geophysical Research 101, 3157-3171.

Planicić, J., Radolić, V., Vuković, B., 2001. Temporal variation of radon in soil related to earthquakes. Applied Radiation and Isotopes 55, 267-272.

Planicić, J., Radolić, V., Vuković, B., 2004. Radon as an earthquake precursor. Nuclear Instruments and Methods in Physics Research, Section A: Accelerators, Spectrometers, Detectors and Associated Equipment 530 (3), 568-574.

Plastino, W., Bella, F., 2001. Radon groundwater monitoring at underground laboratories of Gran Sasso (Italy). Geophysical Research Letters 28, 2675–2678.

Plastino, W., Nisi, S., De Luca, G., Balata, M., Laubenstein, M., Bella, F., 2009. Environmental radioactivity in the ground water at the Gran Sasso National Laboratory (Italy): a possible contribution to the variation of the neutron flux background. Journal of Radioanalytical and Nuclear Chemistry 282 (3), 809-813. doi:10.1007/s10967-009-0151-2.

Plastino, W., Povinec, P.P., De Luca, G., Doglioni, C., Nisi, S., Ioannucci, L., Balata, M., Laubenstein, M., Bella, F., Coccia, E., 2010. Uranium groundwater anomalies and L'Aquila earthquake, 6th April 2009 (Italy). Journal of Environmental Radioactivity 101 (1), 45-50.

Pulinets, S A; Ouzounov, D P; Giuliani, G., Ciraolo, L., Taylor, P.T., 2009. Atmosphere and radon activities observed prior to Abruzzo M6.3 earthquake of April 6, 2009. Eos Trans. AGU 90(52): Abstract AN: U14A-07.

Reddy, D.V., Sukhija, B.S., Nagabhushanam, P., Kumar, D., 2004. A clear case of radon anomaly associated with a micro-earthquake event in a Stable Continental Region. Geophysical Research Letters 31, L10609. doi: 10.1029/2004GL019971.

Richon, P., Sabroux, J.C., Halbwachs, M., Vandemeulebrouck, J., Poussielgue, N., Tabbagh, J., Punongbayan, R., 2003. Radon anomaly in the soil of Taal volcano, the Philippines: a likely precursor of the M 7.1 Mindoro earthquake (1994). Geophysical Research Letters 30 (9), 34-41. doi: 10.1029/2003GL016902.

Richon, P., Perrier, F., Pili, E., Sabroux, J., 2009. Detectability and significance of 12 hr barometric tide in radon-222 signal, dripwater flow rate, air temperature and carbon dioxide concentration in an underground tunnel. Geophysical Journal International 176 (3), 683-694.

Riguzzi, F., Crespi, M., Devoti, R., Doglioni, C., Pietrantonio, G., Pisani, A., 2013. Strain rate relaxation of normal and thrust faults in Italy. Geophysical Journal International 195 (2), 815-820. doi: 10.1093/gji/ggt304.

Rozhnoi, A., Solovieva, M., Molchanov, O., Schwingenschuh, K., Boudjada, M., Biagi, P. F., Maggipinto, T., Castellana, L., Ermini, A., Hayakawa, M., 2009. Anomalies in VLF radio signals prior the Abruzzo earthquake (M=6.3) on 6 April 2009, Natural Hazards Earth System Sciences 9, 1727-1732. doi: 10.5194/nhess-9-1727-2009, 2009.

Sarra, A., Nissi, E., Palermi, S. 2012. Residential radon concentration in the Abruzzo region (Italy): a different perspective for identifying radon prone areas. Environmental and Ecological Statistics, 19 (2), 219-247.

Scholtz, C.H., Sykes, L.R., Aggarval, Y.P., 1973. Earthquake prediction: a physical basis. Science 181, 803-810.

Streil, T., Oeser, V., Feige, S., 2002. An electronic radon dosimeter as a multipurpose device-a bridge between dosimetry and monitoring. Geofisica Internacional 41, 285-288.

Steinitz, G., Begin, Z.B., Gazit-Yaari, N., 2003. Statistically significant relation between radon flux and weak earthquakes in the Dead Sea rift valley. Geology 31 (6), 505-508.

Terakawa, T., Zoporowski, A., Galvan, B., Miller, S.A., 2010. High-pressure fluid at hypocentral depths in the L'Aquila region inferred from earthquake focal mechanisms. Geology 38 (11), 995-998.

Thomas, D.M., Cox, M.E., Cuff, K.E., 1986. The association between ground gas radon variations and geologic activity in Hawaii. Journal of Geophysical Research 91, 12186-12198.

Toutain, J. P., Baubron, J. C., 1999. Gas geochemistry and seismotectonics: a review. Tectonophysics 304, 1–27.

Trique, M., Richon, P., Perrier, F., Avouac, J.P., Sabroux, J.C., 1999. Radon emanation and electric potential variations associated with transient deformation near reservoir lakes. Nature 399, 137-141. doi: 10.1038/20161.

Tuccimei, P., Mollo, S., Vinciguerra, S., Castelluccio, M., Soligo, M., 2010. Radon and thoron emission from lithophysae-rich tuff under increasing deformation: An experimental study. Geophysical Research Letters 37 (5), L05305. DOI: 10.1029/2009GL042134.

Vaupotiĉ, J., Gregoriĉ, A., Kobal, I., Žvab, P., Kozak, K., Mazur, J., Kochowska, E., Grza□dziel, D., 2010. Radon concentration in soil gas and radon exhalation rate at the Ravne Fault in NW Slovenia. Natural Hazards and Earth System Science 10 (4), 895-899.

Wakita H., 1996. Geochemical challenge to earthquake prediction. Proc. Natl. Acad. Sci. USA; 93: 3781-3786

Wyss M. (Ed), 1991. Evaluation of proposed earthquake precursors. Am. Geophys. Union, Washington D.C., 94 pp.

Wyss M., 1997. Second round of evaluations of earthquake precursors. Pure Appl. Geophys., 149: 3-16.

Zmazek, B., Živčić, M., Todorovski, L., Džeroski, S., Vaupotič, J., Kobal, I., 2005. Radon in soil gas: How to identify anomalies caused by earthquakes. Applied Geochemistry 20 (6), 1106-1119.

Figure captions

Fig. 1. Tectonic setting of the L'Aquila region (a) and earthquake location of the 2009 seismic sequence (for seismic events with $M_L > 2$) (b). The location of the mainshock of April 6, 2009 with M_L 5.9 and those major aftershocks of April 7 and April 9, with magnitudes (M_L) of 5.3 and 5.1 respectively, are reported with their focal mechanism solutions (cf. http://cnt.rm.ingv.it/tdmt.html).

The mainshock and the second aftershock are related to pure normal faulting whereas the aftershock of April 7 shows an oblique component due to shearing.

Fig. 2. Comparison between LVD low energy threshold counting rate in s−1 (black) and radon concentrations in Bq/m^3 (gray). Modified after Bruno and Menghetti (2006).

Fig. 3. Sketch of the location of the radon stations together with the site of Laboratori Nazionali del Gran Sasso (LNGS) where LVD tanks are operative. Metereological data were collected by the station at Ponte S. Giovanni nearby the Scoppito village (http://www.caputfrigoris.it). Locations of single stations were plotted onto a Google Earth image.

Fig. 4. Total daily decay counts computed by the two DOSEMan alpha-spectrometers (SARAD Gmbh) of the monitoring stations plotted against particles energy (keV), see text for details. PNG: Paganica station, CPNL: Capannelle Pass station, ARG: Aringo station.

Fig. 5. Large Volume Detector (LVD) low energy traces (~0.8 MeV) collected during the early-mid stages of the seismic sequence compared with earthquakes' magnitude and the daily number of seismic events (with $M_L > 2$). The grey fields indicate the periods when the Laboratories were closed (see text for details).

Fig. 6. Timeseries of radon emissions (^{222}Rn) collected at monitoring stations during our experiment throughout the mid stages of the l'Aquila seismic sequence compared with the histogram of the total number of seismic events. Sampling time was of 4 hours.

Fig. 7. Timeseries of radon concentrations at the Paganica Station (a) compared with soil temperature variations (b). The sampling time was 6 hours for both parameters. Red curves represent daily averages.

Fig. 8. Variation of environmental parameters (atmospheric temperature and pressure, air humidity and rain falls) recorded by the station of Ponte S. Giovanni for the duration of our experiment (http://www.caputfrigoris.it).

Fig. 9. Timeseries of radon concentrations at the Paganica station and display of the residuals. Data were collected with a sampling time of 6 hours; the thick red curve represent daily smoothing

(upper panel). The residuals calculated by means of Multiple Linear Regression (MRL) analysis (i.e., by including the effects of environmental parameters is shown in the lower panel.

Fig. 10. Comparison of the calculated residuals with the sequence of the aftershocks with $M_L>2$ during the exposure time of our automated detector at the PNG station.

Fig. 11. Aftershocks locations plotted onto a Google Earth image during the duration of our experiment. Smaller black dots represent the epicentres of events with $M_L< 3$, whereas lighter green circles are aftershocks with $M_L \geq 3$. Focal mechanism solutions for stronger events are also reported (cf. http://cnt.rm.ingv.it/tdmt.html).

Figure 1
Click here to download high resolution image

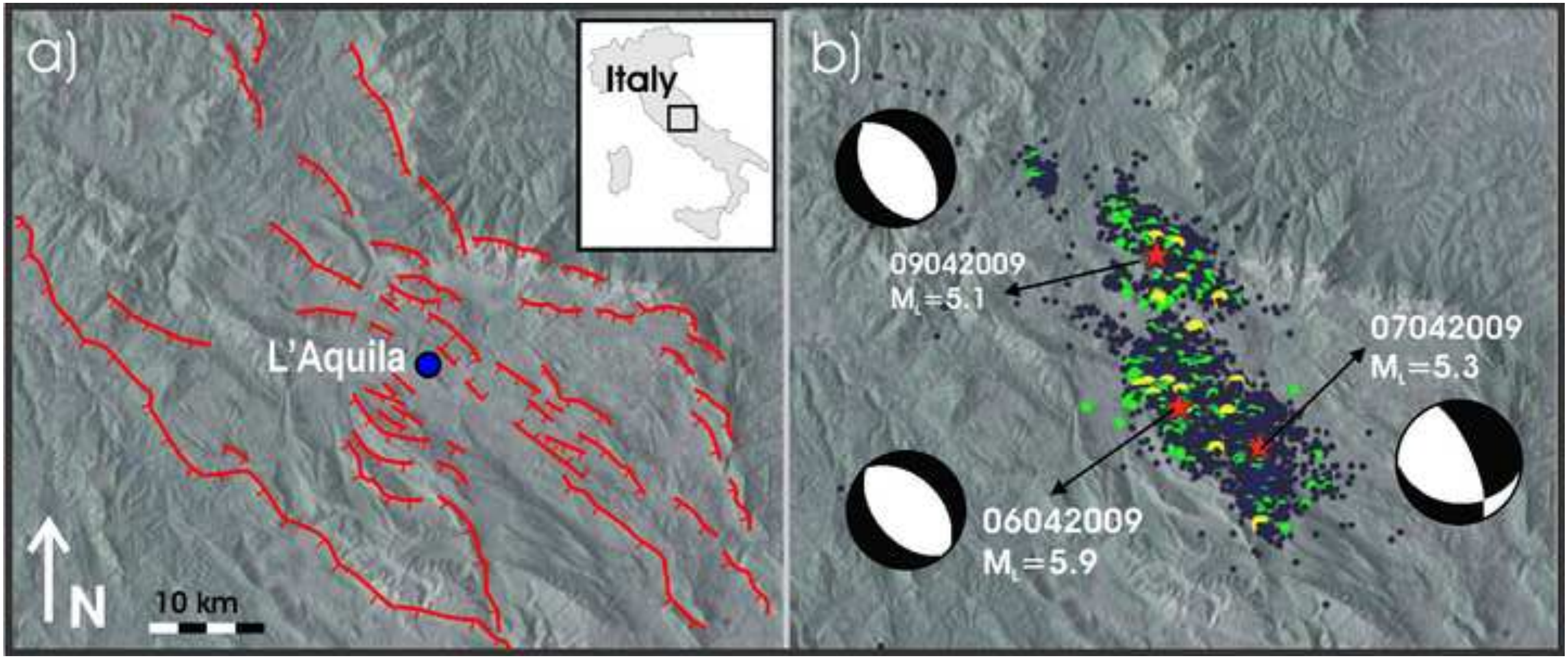

Figure 2
Click here to download high resolution image

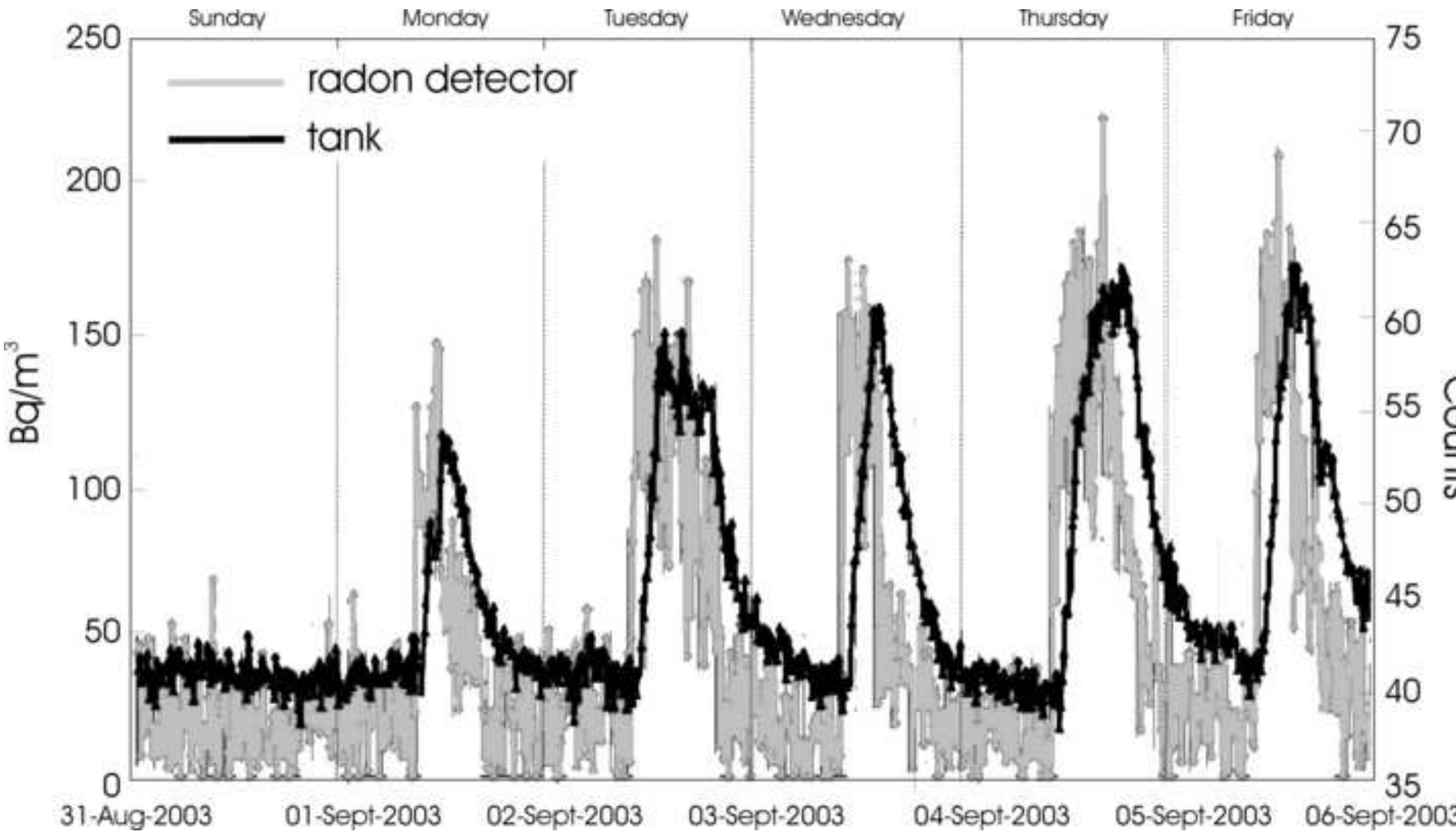

Figure 3
Click here to download high resolution image

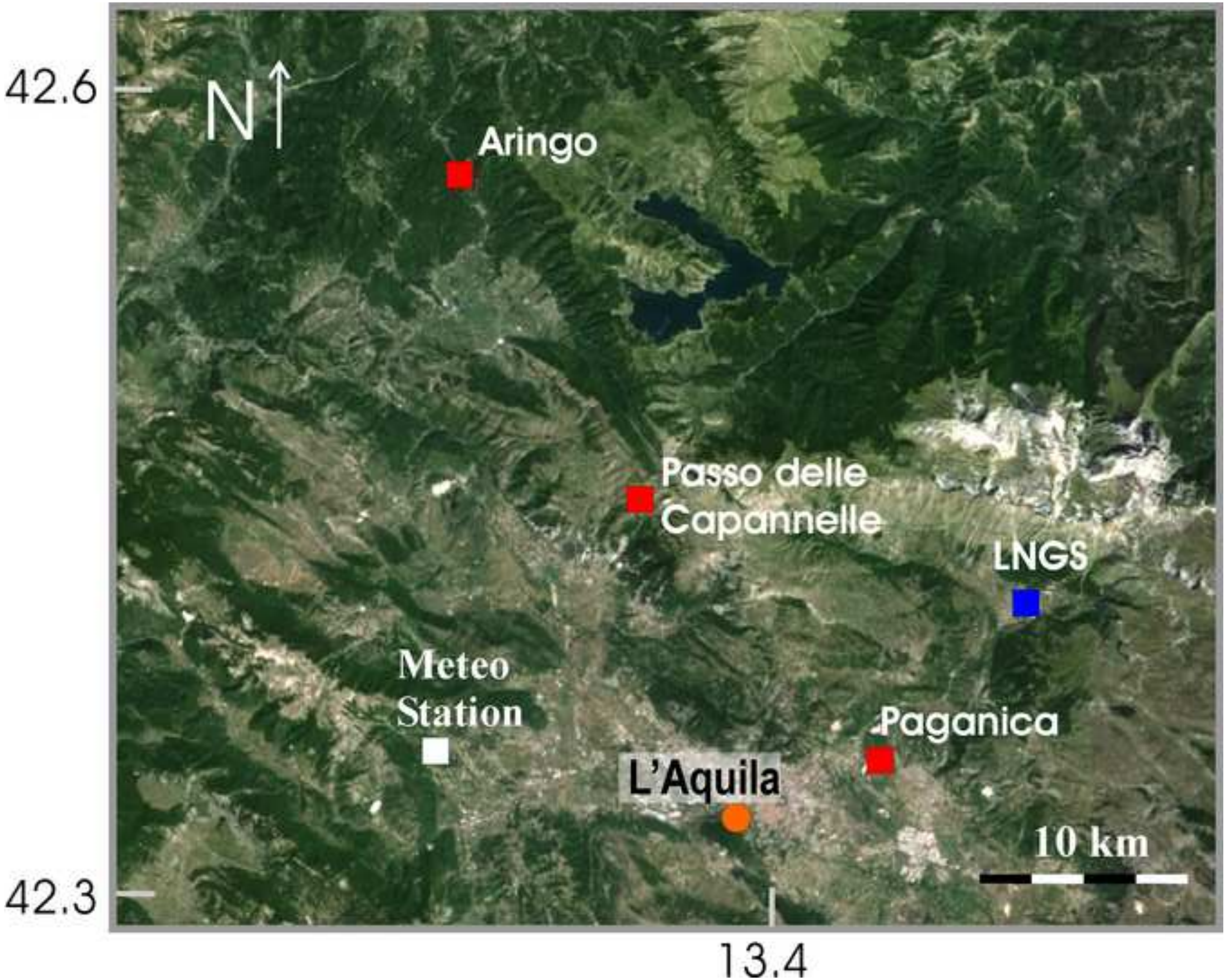

Figure 4
Click here to download high resolution image

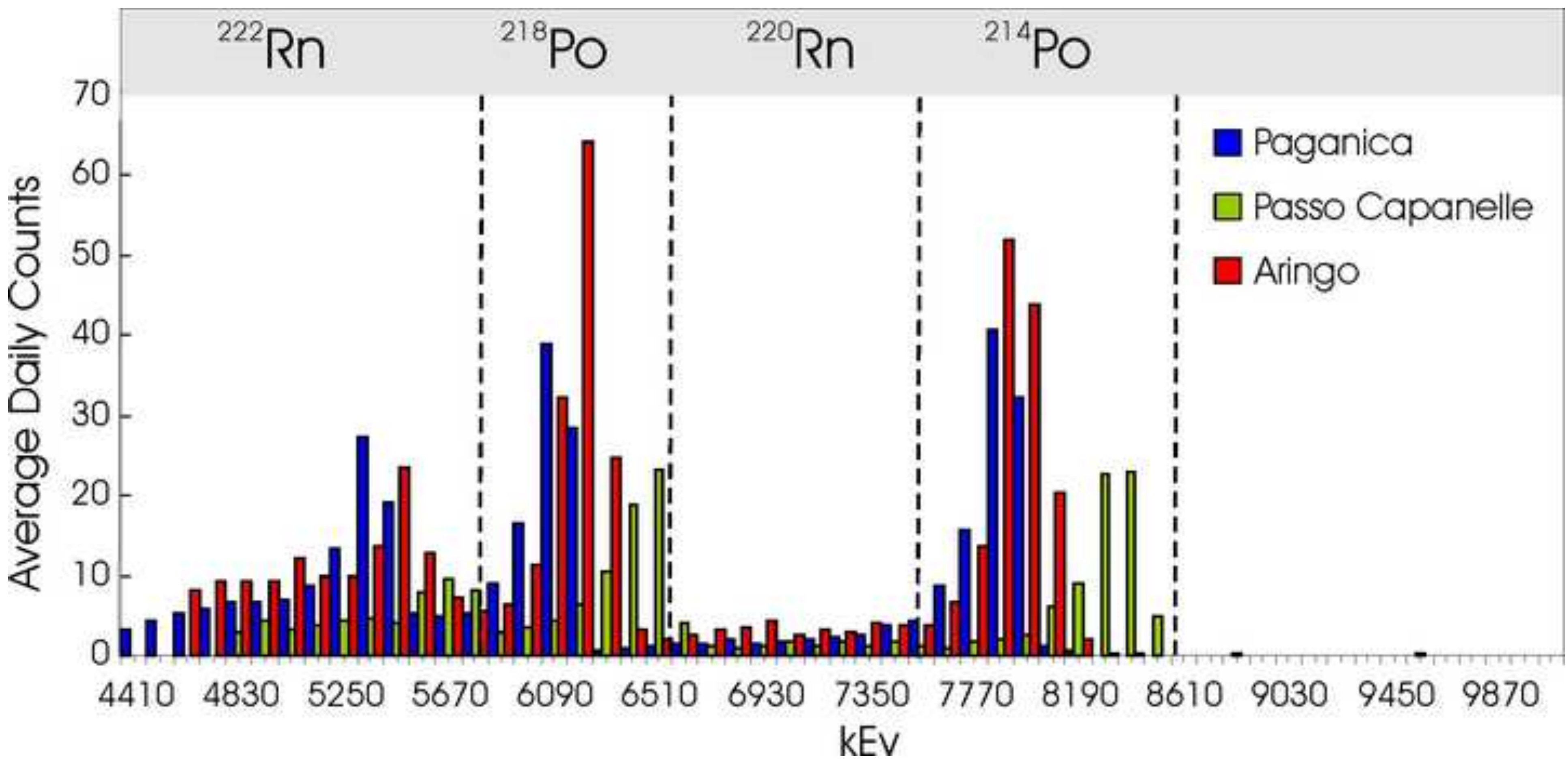

Figure 5
Click here to download high resolution image

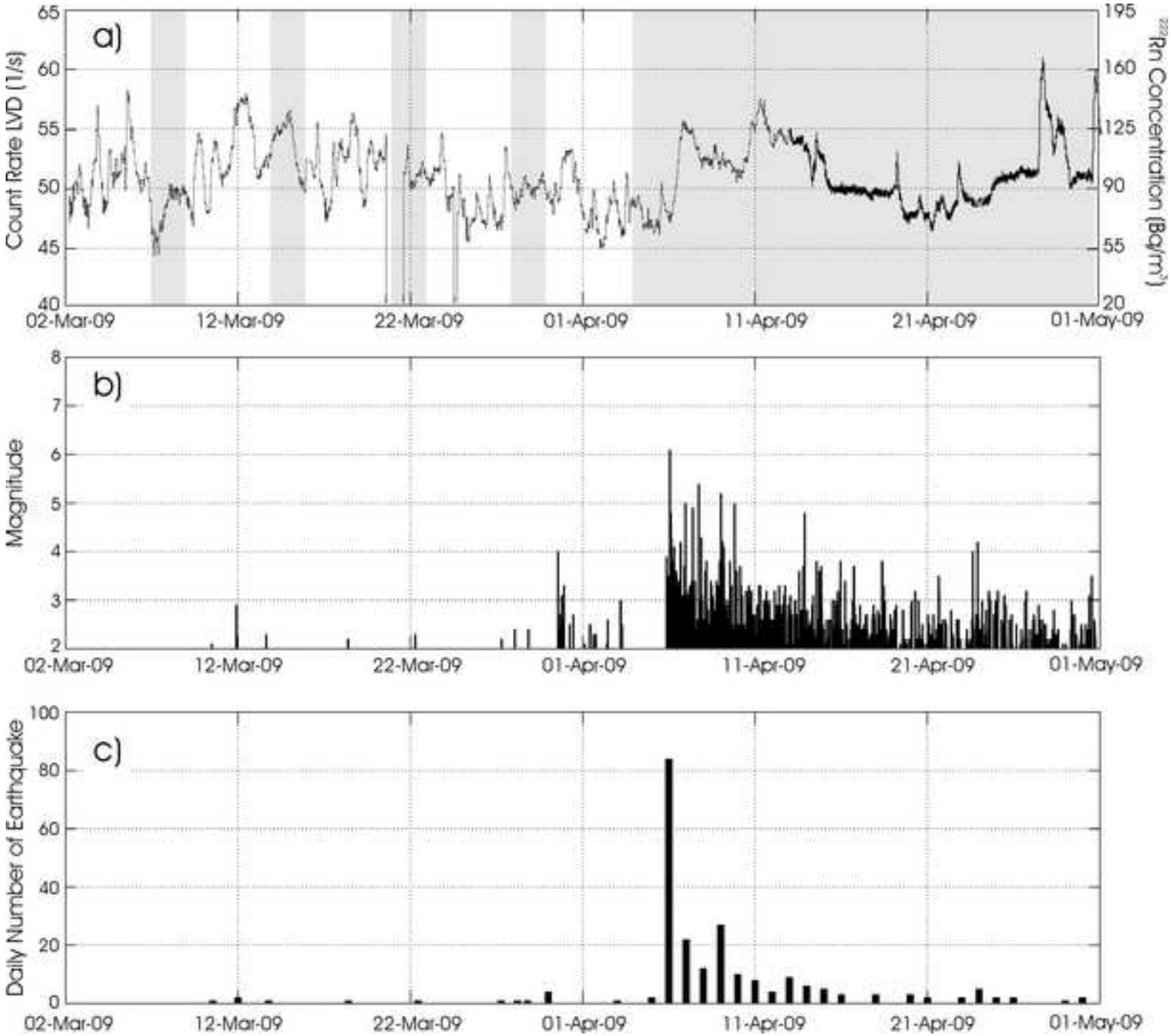

Figure 6
Click here to download high resolution image

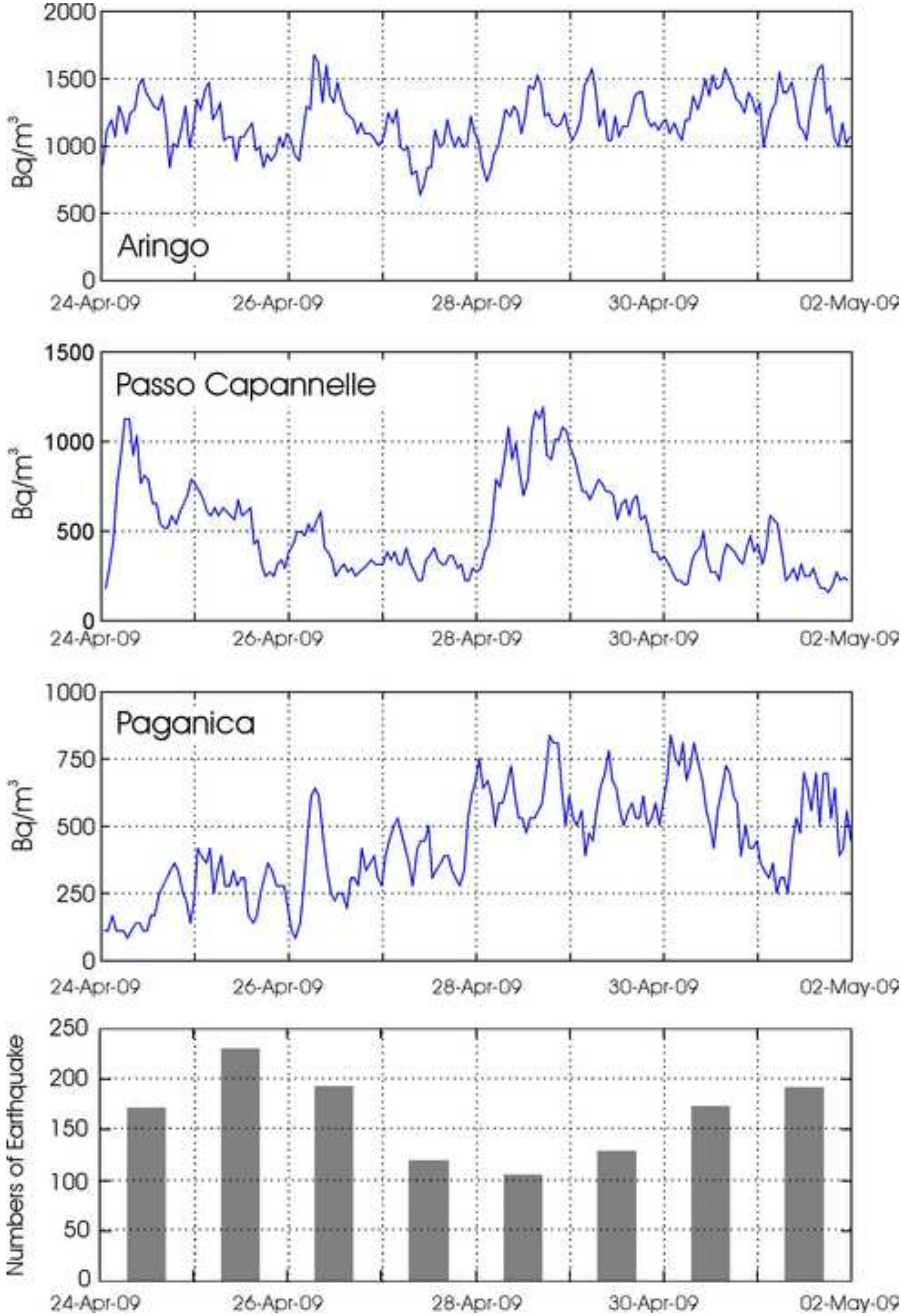

Figure 7
Click here to download high resolution image

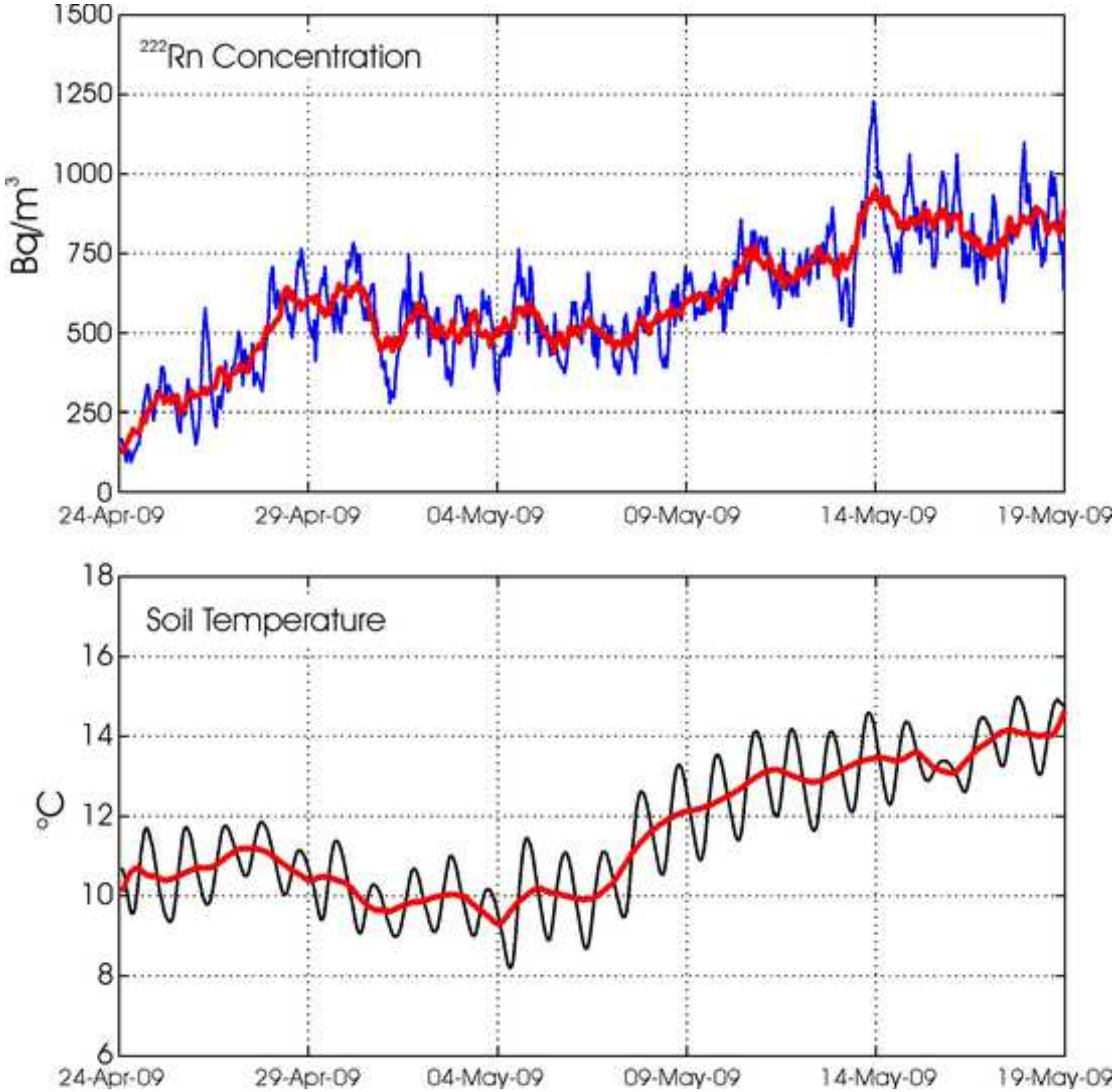

Figure 8
Click here to download high resolution image

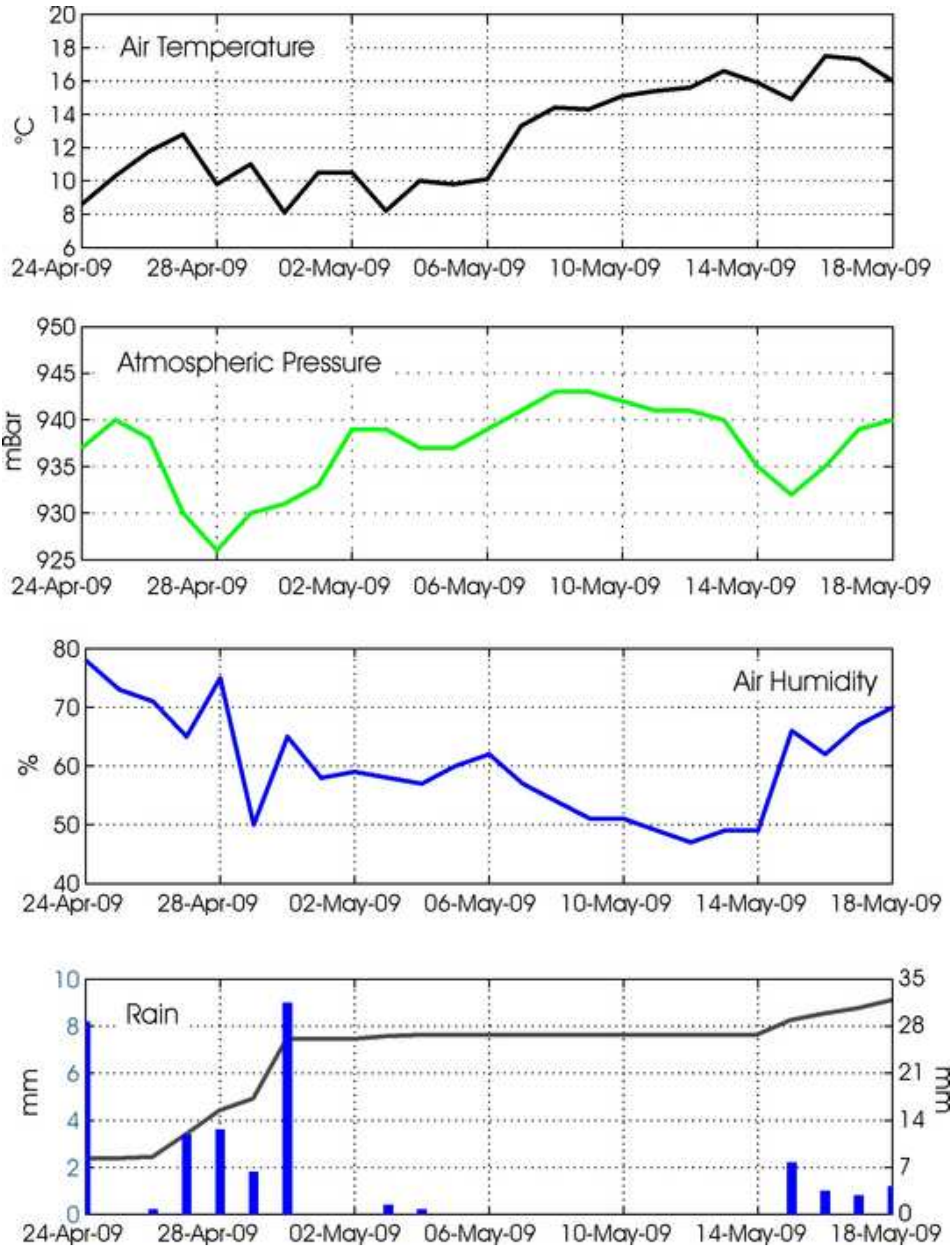

Figure 9

Click here to download high resolution image

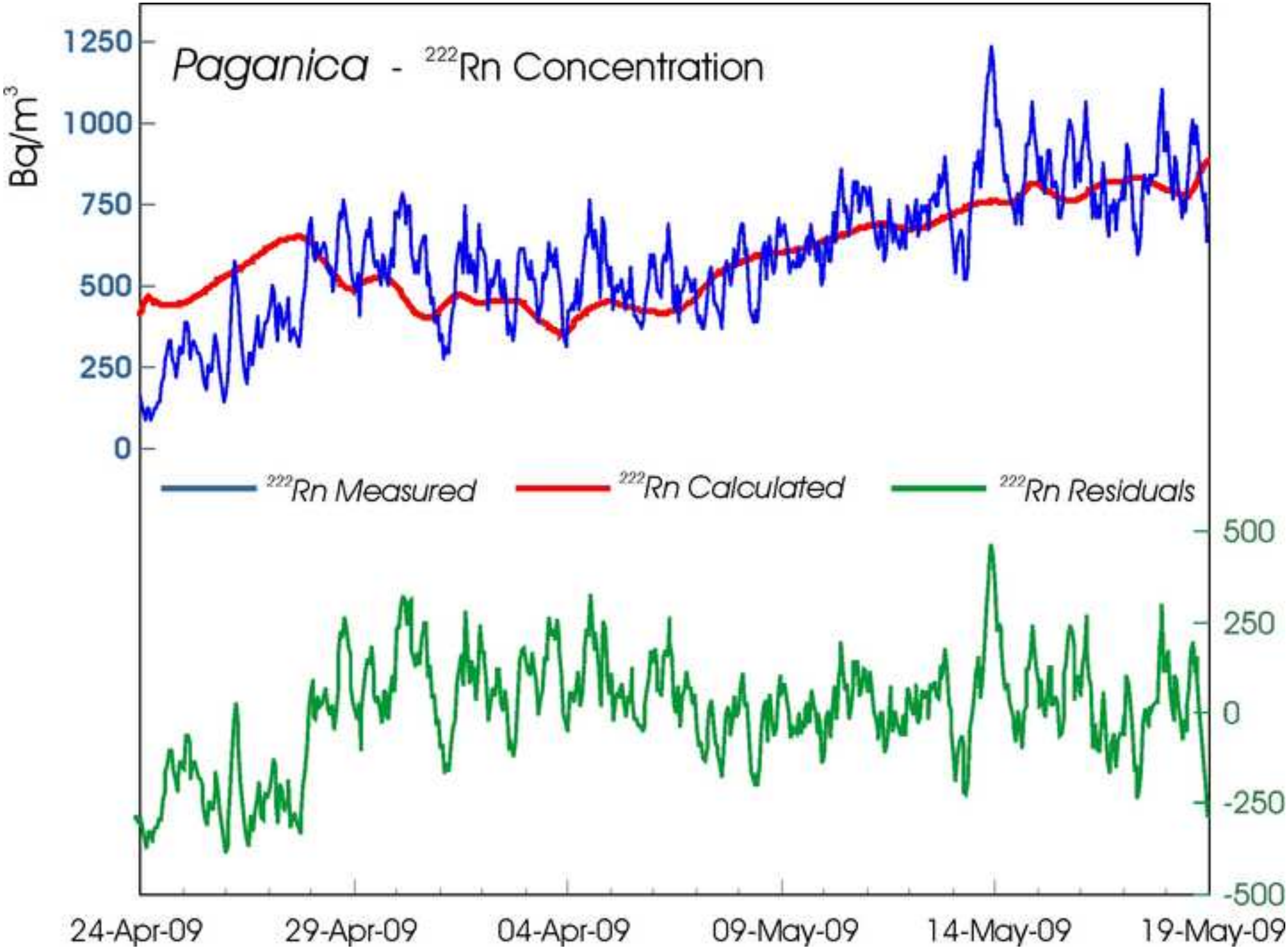

Figure 10

Click here to download high resolution image

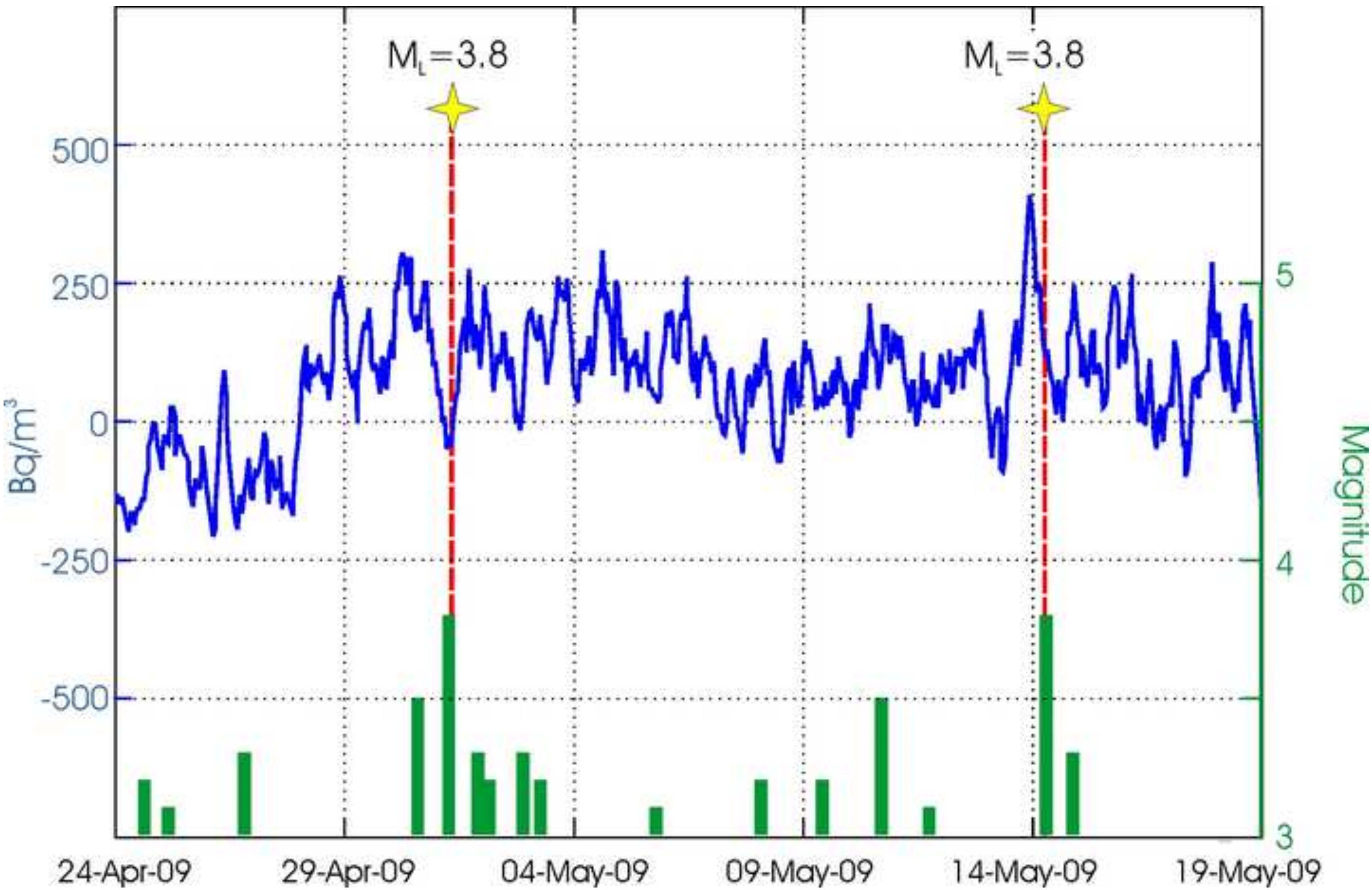

Figure 11
Click here to download high resolution image

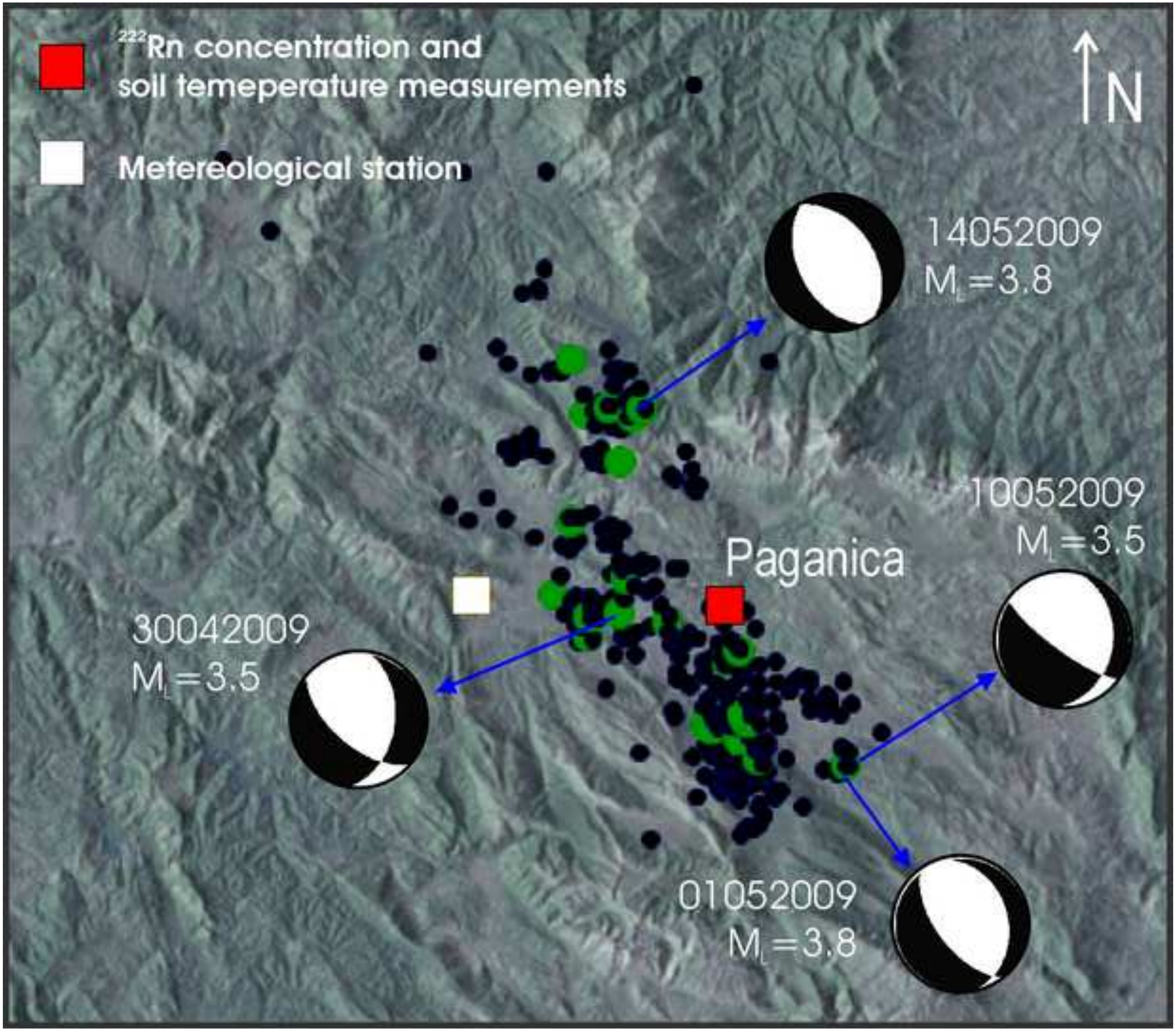

Table 1
Click here to download high resolution image

Table 1. List of the ten higher earthquakes affected the Italian peninsula from the 1900 (INGV; www.ingv.it)

Time	Region	Magnitude (M_w)
28 December 1908	Messina Strict (Calabria, Sicily)	7.2
08 September 1905	Calabria	7.1
13 January 1915	Avezzano (Abruzzo)	7
23 November 1980	Irpinia (Campania,Basilicata)	6.9
23 July 1930	Irpinia (Campania)	6.7
07 September 1920	Garfagnana (Tuscany)	6.5
06 May 1976	Friuli	6.4
06 April 2009	Abruzzo	6.3
29 June 1919	Mugello (Tuscany)	6.2
21 August 1962	Irpinia (Campania)	6.2

Table 2
Click here to download high resolution image

Table 2. Daily correlation coefficients between ^{222}Rn concentration measured at Paganica station (see Figure 3) and the metereological parameters

		^{222}Rn Bq/m^3	Soil T °C	Air T °C	Air Prs mBar	Air H %	Wind Sp km/h
^{222}Rn	Bq/m^3	1.000	0.808	0.705	0.065	-0.263	-0.054
Soil T	°C	0.808	1.000	0.958	0.300	-0.200	-0.123
Air T	°C	0.705	0.958	1.000	0.384	-0.309	-0.044
Air Prs	mBar	0.065	0.300	0.384	1.000	-0.393	0.074
Air H	%	-0.263	-0.200	-0.309	-0.393	1.000	-0.724
Wind Sp	km/h	-0.054	-0.123	-0.044	0.074	-0.724	1.000